

# Continuous production of carbon nanotubes and diamond films by swirled floating catalyst chemical vapour deposition method

A.S. Afolabi<sup>a\*</sup>, A.S. Abdulkareem<sup>a</sup>, S.E. Iyuke<sup>a</sup> and H.C. van Zyl Pienaar<sup>b</sup>

Various techniques for the synthesis of carbon nanotubes (CNTs) are being developed to meet an increasing demand as a result of their versatile applications. Swirled floating catalyst chemical vapour deposition (SFCCVD) is one of these techniques. This method was used to synthesise CNTs on a continuous basis using acetylene gas as a carbon source, ferrocene dissolved in xylene as a catalyst precursor, and both hydrogen and argon as carrier gases. Transmission electron microscopy analyses revealed that a mixture of single and multi-wall carbon nanotubes and other carbon nanomaterials were produced within the pyrolytic temperature range of 900–1100°C and acetylene flow rate range of 118–370 ml min<sup>-1</sup>. Image comparison of raw and purified products showed that low contents of iron particles and amorphous carbon were contained in the synthesised carbon nanotubes. Diamond films were produced at high ferrocene concentration, hydrogen flow rate and pyrolysis temperatures, while carbon nanoballs were formed and attached to the surface of the CNTs at low ferrocene content and low pyrolysis temperature.

**Key words:** SFCCVD, CNTs, continuous production, pyrolysis, diamond films

## Introduction

Carbon nanotubes (CNTs) are poised to make themselves the 'materials of the millennium' due to their unique characteristics, such as good mechanical properties<sup>1,2</sup> good electrical conductivity<sup>3-5</sup> and other special functional properties,<sup>6,7</sup> which have culminated in various technological developments in recent times. The exceptional properties of these 'miracle materials', as they are called by Karel,<sup>8</sup> have provoked the interest of many researchers, scientists and technologists from all parts of the world. Some of the applications of these materials are energy storage,<sup>9</sup> hydrogen storage,<sup>10-12</sup> field emission,<sup>13</sup> nanoelectric devices,<sup>14</sup> artificial muscle,<sup>15</sup> reinforcing materials<sup>16</sup> and catalyst support in fuel cells.<sup>17,18</sup> This versatility in the applications of CNTs places their price in the international market as high as five hundred U.S. dollars per gram.

Since CNTs were discovered by Iijima,<sup>19</sup> various methods for their production have been developed.<sup>20-24</sup> The chemical vapour deposition (CVD) method has been identified as the best for large-scale production of the materials.<sup>25,26</sup> In the same vein, many other carbon nanomaterials are usually associated with the CVD production technique; some of these nanomaterials are

carbon nanoballs,<sup>27</sup> carbon nanofibres,<sup>28</sup> carbon nanorods<sup>29</sup> and even diamond particles.<sup>30</sup>

Chemical vapour deposition production of CNTs has employed different carbon and catalyst sources<sup>31-33</sup> which have significant effects on the type and quality of CNTs produced. This paper presents another CVD technique termed swirled floating catalyst chemical vapour deposition (SFCCVD) which employs acetylene as the carbon source and ferrocene dissolved in xylene as the catalyst precursor to produce CNTs on a continuous basis. The analyses of these products revealed that the mixture of single- and multi-walled carbon nanotubes produced were of high purity. Diamond films were also produced alongside these materials.

## Methods

The apparatus used for the production of CNTs was developed by Iyuke,<sup>34</sup> presented schematically in Fig. 1. The equipment consisted of a vertical silica plug flow reactor (1) immersed in a furnace (2) with a sensitive temperature regulator, and a system of rotameters, pressure controllers and valves that controlled the flow of hydrogen, nitrogen, argon and acetylene gases into the reactor. The upper end of the reactor was connected to a condenser (3) which led to two delivery cyclones (4 and 5) where the CNTs produced were collected. The ferrocene catalyst was dissolved in xylene at specific quantities and pumped (8) at regular intervals into a ferrocene vaporiser (6) placed on a heater with a sensitive temperature regulator. This catalyst vaporiser was connected to the swirled mixer (7) which in turn led into the reactor.

Nitrogen was first turned on to purge the system of any impurity. The reactor and ferrocene heater were switched on while the nitrogen was running. At a reactor temperature of about 300°C, nitrogen was turned off to prevent it from reacting with oxygen. Argon was then turned on at a prescribed flow rate to continue purging and to act as a carrier gas. At reactor temperatures of 900°C, 950°C, 1000°C, 1050°C and 1100°C, and a catalyst heater temperature of 150°C, ferrocene dissolved in xylene was pumped into the vaporiser at intervals while hydrogen and acetylene gases were turned on at specified flow rates. The system was run continuously while the catalyst was pumped into the vaporiser at regular intervals. The smoky product, or carbon vapour emitted from the reactor, was cooled at the condenser and collected in the cyclones. The wall of the reactor was also scraped clean of CNTs. These raw CNTs were treated with 30% HNO<sub>3</sub> and stirred for 2 h at room temperature. The

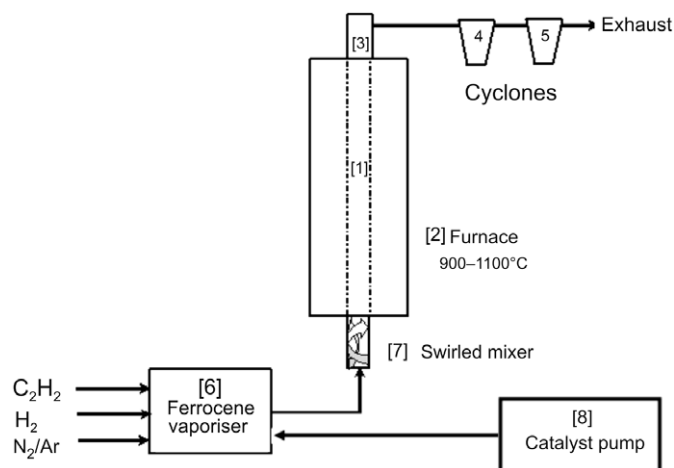


Fig. 1. Schematic of the swirled floating catalyst chemical vapour deposition reactor.<sup>33</sup>

<sup>a</sup>School of Chemical and Metallurgical Engineering, Faculty of Engineering and the Built Environment, University of the Witwatersrand, Private Bag X3, WITS 2050, South Africa.

<sup>b</sup>Institute of Applied Electronics, Faculty of Engineering and Technology, Vaal University of Technology, Private Bag X021, Vanderbijlpark 1900, South Africa.

\*Author for correspondence E-mail: afolabisammy@yahoo.com

solid products were filtered, washed repeatedly with distilled water until a pH of 7 was achieved, and dried at 120°C in hot air for 12 h. The as-synthesised and purified samples were analysed and characterised. A JSM 840 scanning electron microscope (SEM) and a high-resolution transmission electron microscope (HRTEM, Philips CM200) were used to investigate the surface morphology of both as-synthesised and purified carbon nanomaterial samples. A trace amount of each of these samples was ultrasonically vibrated in methanol until they were well dispersed and formed a suspension in the solvent. A drop of this suspension was spread on a 300-mesh copper grid with lacy carbon thin film and allowed to dry. After drying, the grid was loaded into the instrument for TEM operation using 100 keV. X-ray diffraction (XRD) patterns of the products were recorded by a Philips X Pert X-ray diffractometer with graphite monochromatised copper  $K\alpha$ -radiation.

### Results and discussion

The SFCCVD method was used to synthesise various carbon nanomaterials at different flow rates of the carbon source (acetylene) and carrier gas (hydrogen), and different catalyst concentrations (based on the percentage of ferrocene dissolved in xylene). Figure 2a shows the image of as-synthesised single-walled carbon nanotubes (SWCNTs) obtained at a concentration of 10% ferrocene, a pyrolysis temperature of 1 100°C and an acetylene flow rate of 248 ml min<sup>-1</sup>. This sample contained traces of iron impurities trapped within the tubes. This was due to excess iron particles that could not form nucleation sites for carbon nanotube growth. The image of a purified SWCNT shown in Fig. 2b reveals that the acid treatment removed the iron impurities in the tubes. The two images show little or no amorphous carbon. The images of as-synthesised and purified multi-walled carbon nanotubes (MWCNTs), produced at 3% ferrocene and 1 000°C, are shown in Figs 3a and 3b, respectively. Comparing these samples, it can be seen that both contained trace amounts of both iron impurities and amorphous carbon. This could be attributed to the limit of solubility of ferrocene in xylene at room temperature.<sup>35</sup> This supports the finding of Liu *et al.*<sup>35</sup> that at low ferrocene concentrations, the catalysis efficiency of ferrocene is high. Though the quantity of CNTs produced at lower ferrocene concentrations was small, the low amorphous carbon and iron particles in the samples resulted in formation of clean CNTs. The effects of ferrocene concentration and pyrolysis temperature on the rate of production of carbon nanomaterials are presented in sections 3.1 and 3.2, respectively.

#### Effect of ferrocene concentration

The ferrocene catalyst was the precursor for iron particles which acted as the nucleation sites for the growth of CNTs. Xylene was used as a solvent to dissolve the ferrocene for easy transportation into the heater and also functioned as a CNT growth promoter. Figure 4a shows the SEM image of clustered CNTs produced at a ferrocene concentration of 3% and a pyrolysis temperature of 1 050°C. Figure 4b presents the TEM image of the carbon nanoballs (indicated by the arrows) obtained at a

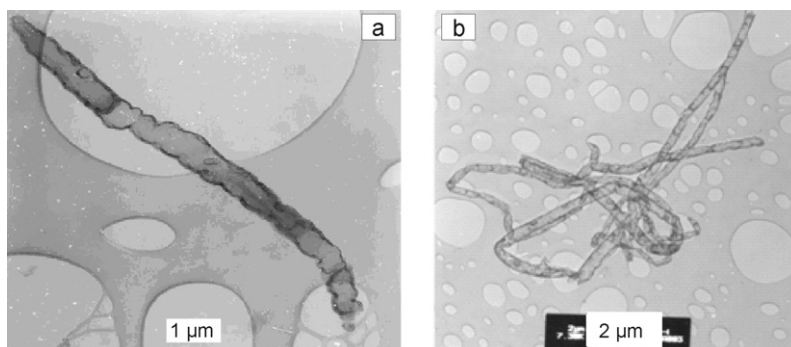


Fig. 2. High-resolution transmission electron microscopy images of (a) as-synthesised SWCNT obtained at 10% ferrocene and 1 100°C and (b) purified SWCNT obtained at 5% ferrocene and 1 000°C.

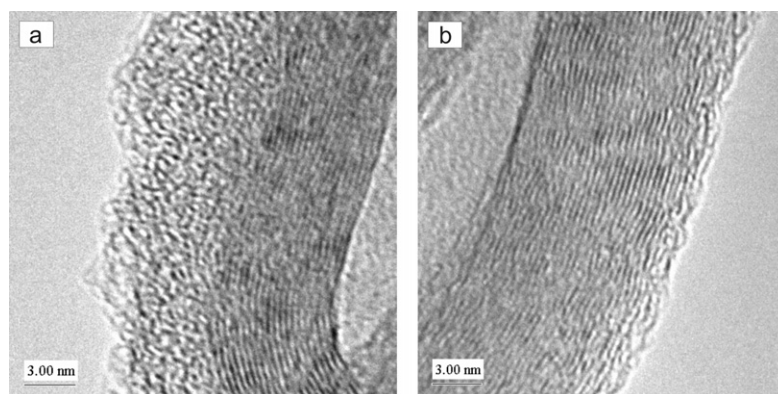


Fig. 3. Transmission electron microscopy images of (a) as-synthesised and (b) purified MWCNTs obtained at 3% ferrocene and 1 000°C.

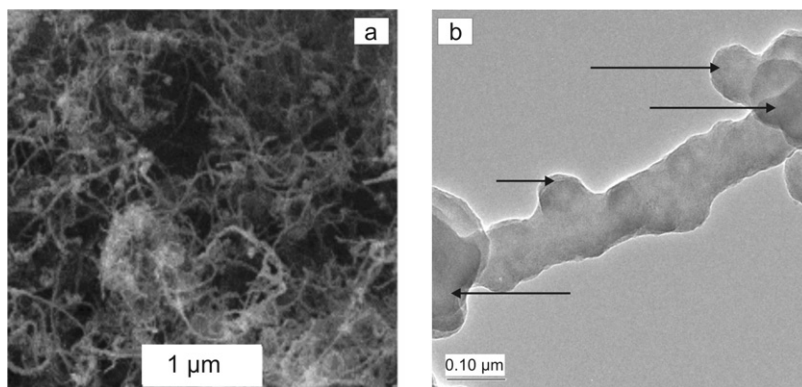


Fig. 4. (a) Scanning electron microscopy image of clustered CNTs obtained at 3% ferrocene concentration and 1 050°C and (b) transmission electron microscopy image of carbon nanoballs obtained at 2% ferrocene concentration and 900°C (arrows point to carbon nanoballs).

ferrocene concentration of 2% and a pyrolysis temperature of 900°C. These carbon nanoballs were formed due to a low content of ferrocene at low pyrolysis temperature, as reported by Liu *et al.*<sup>35</sup> The xylene might have assisted in the formation of these carbon nanoballs since low catalyst content at high temperature is known to result in CNTs with a high content of amorphous impurities. Figure 5 shows that varying the concentration of ferrocene had a significant effect on the production rate of carbon nanomaterials. It can be seen that the highest production rate of 0.36 g min<sup>-1</sup> was obtained at a 10 wt% concentration of ferrocene in xylene and an acetylene flow rate of 248 ml min<sup>-1</sup> at 1 100°C.

#### Effect of pyrolysis temperature

The effect of pyrolysis temperature on the rate of production of carbon nanomaterials at various flow rates of acetylene, various

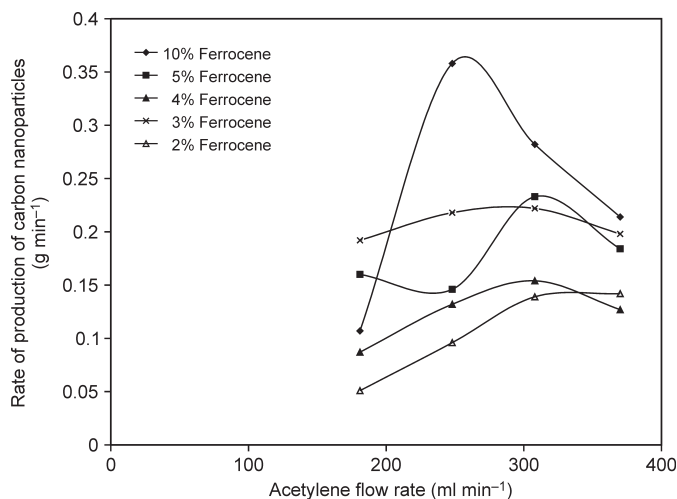


Fig. 5. Effect of ferrocene concentration on the rate of production of carbon nanomaterials at different acetylene flow rates.

concentrations of ferrocene and a constant hydrogen flow rate of 181 ml min<sup>-1</sup> is shown in Fig. 6. Attempts were made to produce carbon nanoparticles at lower temperatures (750–850°C) but no products were obtained. The pyrolysis temperatures were therefore varied between 900°C and 1 100°C. The rate of production of carbon nanomaterials was significantly affected by the pyrolysis temperature as well as the acetylene flow rate. The highest production rate was observed at 1 100°C, at an acetylene flow rate of 248 ml min<sup>-1</sup>.

#### Production of diamond films

At an acetylene flow rate of 248 ml min<sup>-1</sup>, hydrogen flow rate of 181 ml min<sup>-1</sup> and pyrolysis temperatures between 1 000°C and 1 100°C, diamond particles as well as glassy carbon were produced alongside CNTs. The production of these diamond particles (Figs 7a and 7b) could be attributed to the ionisation of hydrogen gas at high temperatures. The diamond films were however, thermodynamically unstable as they disappeared after a few minutes. Figure 8 shows the XRD analysis of the samples obtained at a temperature of 1 000°C, an acetylene flow rate of 248 ml min<sup>-1</sup>, hydrogen flow rate of 181 ml min<sup>-1</sup>, and 10 wt% and 2 wt% concentrations of ferrocene, respectively. The analysis confirms the presence of diamond flakes and glassy carbon identified as graphite nitrate; the nitrogen in the nitrate may have been from the traces contained in the argon and hydrogen gases (Afrox), which were 4 and 2 volume per million (Vpm), respectively.

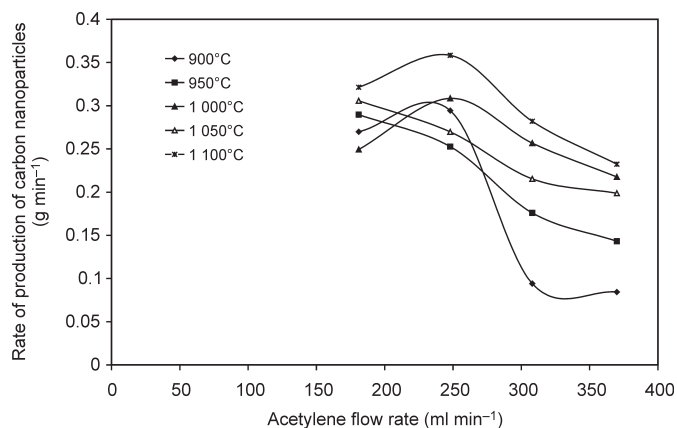


Fig. 6. Effect of pyrolysis temperature on the rate of production of carbon nanomaterials at different acetylene flow rates.

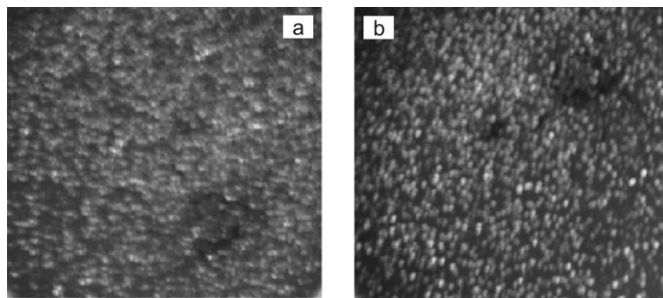


Fig. 7. Photographic images (EuroTEK 10 Megapixels) of diamond films obtained at (a) 10% ferrocene, 1 000°C and a hydrogen flow rate of 118 ml min<sup>-1</sup>, and (b) 10% ferrocene, 1 100°C and a hydrogen flow rate of 181 ml min<sup>-1</sup>.

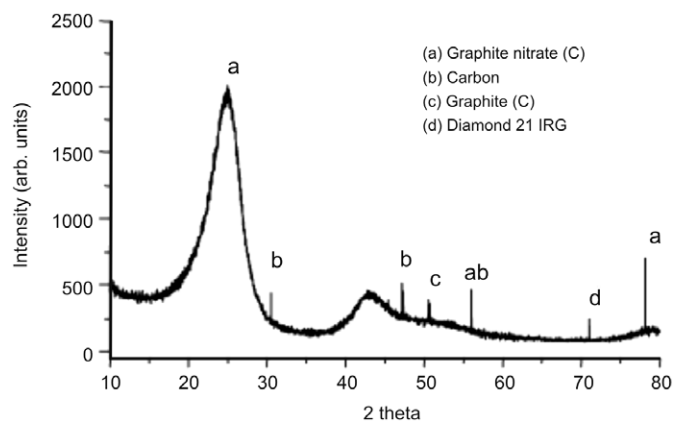


Fig. 8. X-ray diffraction analysis of a sample produced at 10% ferrocene, 1 100°C and a hydrogen flow rate of 181 ml min<sup>-1</sup>, confirming traces of diamond films.

It was observed that the rate of production of diamond films increased with increases in the concentration of ferrocene, hydrogen flow rate and pyrolysis temperature. These parameters play significant roles in the quality of synthesised CNTs and are therefore contributing factors in the formation of these diamond particles.<sup>36</sup> The excess iron impurity in the synthesised CNTs might have been responsible for the nucleation of diamond which grew at high pyrolysis temperature. Carbon nanotubes containing high amounts of amorphous carbon as the nucleation precursor will produce graphite, rather than diamond, at the pyrolysis temperatures studied due to graphite's lower energy state.<sup>37</sup> However, the trace amount of amorphous carbon in the CNTs produced possibly makes the iron catalyst lose its activity, leading to the formation of diamond films with less developed morphology. The thermodynamic stability, morphology and crystal size of these diamond films are still under study.

#### Conclusion

The SFCCVD method presents a novel, continuous synthesis of both single- and multi-walled carbon nanotubes, as well as other nanomaterials, with a maximum production rate of 0.36 g min<sup>-1</sup> which allows mass production of these materials and presents a breakthrough in the production of CNTs. These CNTs contained trace amounts of iron impurities and amorphous carbon. Diamond films were formed at high ferrocene concentrations, hydrogen flow rate and pyrolysis temperatures, while carbon nanoballs were formed at low ferrocene concentration and pyrolysis temperature. The higher the acetylene flow rate, the higher the rate of production of these nanomaterials.

The financial support provided by the Wits University Research Council (URC) Equipment grant, Centre of Excellence in Strong Materials (CoE-SM) and the Vaal

University of Technology is much appreciated. The technical support given by the Wits Microscopy and Microanalysis Unit and Willie Augustyn of the Tshwane University of Technology is also appreciated.

Received 18 May. Accepted 29 July 2009.

1. Treacy M.M.J., Ebbesen T.W. and Gibson J.M. (1996). Exceptionally high Young's modulus observed for individual carbon nanotubes. *Nature* **381**, 678–680.
2. Lu J.P. (1997). Elastic properties of carbon nanotubes and nanopores. *Phys. Rev. Lett.* **79**, 1297–1300.
3. Song S.N., Wang X.K., Chang R.P.H. and Ketterson J.B. (1994). Electronic properties of graphite nanotubes from galvanomagnetic effects. *Phys. Rev. Lett.* **72**, 697–700.
4. Sanvito S., Kwon Y., Tománek D. and Lambert C.J. (2000). Fractional quantum conductance in carbon nanotubes. *Phys. Rev. Lett.* **84**, 1974.
5. Kociak M., Kasumov A.Y., Gueron S., Reulet B., Khosdos I.I. and Gorbatov Y.B. (2001). Superconductivity in ropes of single-walled carbon nanotubes. *Phys. Rev. Lett.* **86**, 2416–2419.
6. Hone J., Whitney M. and Zettle A. (1999). Physical properties of carbon nanotubes. *J. Synth. Metals* **103**, 2498.
7. Che J., Cagin T. and Goddard W.A. (2000). Thermal conductivity of carbon nanotubes. *Nanotech.* **11**, 65–69.
8. Karel S. (2006). Carbon nanotubes now used on an industrial scale. *Eng. News* **26**(30), 81.
9. Che G., Lakshmi B.B., Martin C.R. and Fisher E.R. (1999). Metal-nanocluster-filled carbon nanotubes: catalytic properties and possible applications in electrochemical energy storage and production. *Langmuir* **15**, 750–758.
10. Dillon A.C., Jones K.M., Bekkedahl T.A., Kiang C.H., Bethune D.S. and Heben M.J. (1997). Storage of hydrogen in single carbon nanotubes. *Nature* **386**, 377–379.
11. Nutzenadel C., Zuttel A., Chartouni D. and Schlögl L. (1999). Electrochemical storage of hydrogen in nanotube materials. *Electrochem. Solid-State Lett.* **2**, 30–32.
12. Liu C., Fan Y.Y., Liu M., Cong H.T., Cheng H.M. and Dresselhaus M.S. (1999). Hydrogen storage in single-walled carbon nanotubes at room temperature. *Science* **286**, 1127–1129.
13. Yumura M., Ohshima S., Uchida K., Tasaka Y., Kuriki Y., Ikazaki F., Saito Y. and Uemura S. (1999). Synthesis and purification of multi-walled carbon nanotubes for field emitter applications. *Diam. Relat. Mater.* **8**, 785–791.
14. Hoenlein W., Kreupl F., Duesberg G.S., Graham A.P., Liebau M., Seidel R. and Unger E. (2003). Carbon nanotubes for microelectronics: status and future prospects. *Mater. Sci. Eng. Biomim. Mater. Sens. Syst.* **23**, 663–669.
15. Heer W.A.D., Chatelain A. and Ugarte D. (1995). A carbon nanotubes field-emission electron source. *Science* **270**, 1179–1180.
16. Shaffer M. (2004). Prospects for nanotubes and nanofibre composites. *Compos. Sci. Technol.* **64**, 2281–2282.
17. Rajesh B., Karthik V., Karthikeyan S., Thampi R.K., Bonard J.M. and Viswanathan B. (2002). Pt-WO<sub>3</sub> supported on carbon nanotubes as possible anodes for direct methanol fuel cells. *Fuel* **81**, 2177–2190.
18. Matsumoto T., Komatsu T., Nakano H., Arai K., Nagashima Y., Yoo E., Yamazaki T., Kijima M., Shimizu H., Takasawa Y. and Nakamura J. (2004). Efficient usage of highly dispersed Pt on carbon nanotubes for electrode catalysts of polymer electrolyte fuel cells. *Catal. Today* **90**, 277–281.
19. Iijima S. (1991). Helical microtubules of graphitic carbon. *Nature* **354**, 56–58.
20. Seraphin S. and Zhou D. (1994). Single-walled carbon nanotubes produced at high yield by mixed catalysts. *Appl. Phys. Lett.* **64**, 2087–2089.
21. Lambert J.M., Ajayan P.M., Bernier P., Planeix J.M., Brotons V. and Coq B. (1994). Improving conditions towards isolating single-shell carbon nanotubes. *Chem. Phys. Lett.* **226**, 364–371.
22. Cheng H.M., Li F., Sun X., Brown S.D.M., Pimenta M.A. and Marucci A. (1998). Bulk morphology and diameter distribution of single-walled carbon nanotubes synthesized by catalytic decomposition of hydrocarbons. *Chem. Phys. Lett.* **289**, 602–610.
23. Master W.K., Munoz E., Benito A.M., Martinez M.T., de La Fuente G.F. and Maniette Y. (1998). Production of high-density single-walled nanotube materials by a simple laser ablation method. *Chem. Phys. Lett.* **99**, 10694–10697.
24. Kingston C.T., Jakubek Z.J., Denomme S. and Simard B. (2004). Efficient laser synthesis of single-walled carbon nanotubes through laser heating of the condensing vaporization plume. *Carbon* **42**, 1657–1664.
25. Conteau E., Hernadi K., Seo K., Seo J.W., Thien-Nga L., Miko C.S., Gaal R. and Forro L. (2003). CVD synthesis of high purity carbon nanotubes using CaCO<sub>3</sub> catalyst support for large scale production. *Chem. Phys. Lett.* **378**, 9–17.
26. Kathyayini H., Nagaraju N., Fonseca A. and Nagy J.B. (2004). Catalytic activity of Fe, Co and Fe/Co supported on Ca and Mg oxides, hydroxide in the synthesis of carbon nanotubes. *J. Mol. Catal.* **223**, 129–136.
27. Zhong Z., Chen H., Tang S., Ding J., Lin J. and Tan K.L. (2000). Catalytic growth of carbon nanoballs with and without cobalt encapsulation. *Chem. Phys. Lett.* **330**, 41–47.
28. Endo M., Kim Y.A., Hayashi T., Nishimura K. and Matusita T. (2001). Vapour-grown carbon fibres (VGCf): basic properties and their battery applications. *Carbon* **39**, 1287–1297.
29. Liu Y., Hu W., Wang X., Long C., Zhang J., Zhu D., Tang D. and Xie S. (2000). Carbon nanorods. *Chem. Phys. Lett.* **331**, 31–34.
30. Zhang F., Shen J., Sun J. and McCartney D.G. (2006). Direct synthesis of diamond from low purity carbon nanotubes. *Carbon* **44**(14), 3136–3138.
31. Kuwana K., Endo H., Saito K., Qian D., Andrews R. and Grulke E.A. (2005). Catalytic deactivation of carbon nanotubes. *Carbon* **43**, 252–260.
32. Wang Y., Wei F., Gu G. and Yu H. (2002). Agglomerated carbon nanotubes and its mass production in a fluidized-bed reactor. *Physica B* **323**, 327–329.
33. Iyuke S.E. and Danna A.B.M. (2005). Morphological study of carbon nanotubes synthesized by FCCVD. *Microporous Mesoporous Mater.* **84**, 338–342.
34. Iyuke S.E. (2007). *A Process for Producing Carbon Nanotubes*. PCT application WO 2007/026213 (Published 2007/03/08) priority data ZA 2005/03438 2005/08/29.
35. Liu X.Y., Huang B.C. and Coville N.J. (2002). The Fe(CO)<sub>5</sub> catalyzed pyrolysis of pentane: carbon nanotubes and carbon nanoballs formation. *Carbon* **40**, 2791–2799.
36. Hou Y.Q., Zhuang D.M., Zhang G., Wu M.S. and Liu J.J. (2002). Preparation of diamond films by hot filament chemical vapour deposition and nucleation by carbon nanotubes. *Appl. Surf. Sci.* **185**, 303–308.
37. Wang Q.S. (2002). *Fabrication of Superhard Materials*, pp. 122–125. Standards Press of China, Beijing.